

## Supporting Information

### **Trace Water Accelerating the CO<sub>2</sub> Cycloaddition Reaction Catalyzed by Indium-Organic Framework**

Sheng-Li Hou,<sup>a</sup> Jie Dong,<sup>a</sup> Zhuo-Hao Jiao,<sup>a</sup> Xiao-Lei Jiang,<sup>a</sup> Xiu-Pei Yang,<sup>\*b</sup>  
Bin Zhao<sup>\*a</sup>

<sup>a</sup> College of Chemistry, Key Laboratory of Advanced Energy Material Chemistry, MOE, and Collaborative Innovation Center of Chemical Science and Engineering (Tianjin), Nankai University, Tianjin 300071, China. \*E-mail: [zhaobin@nankai.edu.cn](mailto:zhaobin@nankai.edu.cn). Fax: 86-022-23502458.

<sup>b</sup> College of Chemistry and Chemical Engineering, China West Normal University, Nanchong 637000, China. \*E-mail: [xiupeiyang@163.com](mailto:xiupeiyang@163.com)

Sheng-Li Hou and Jie Dong contributed equally to this work.

Table of contents:

Section S1. Materials and Characterization.....	S-2
Section S2. Experimental Section.....	S-2
Section S3. References.....	S-3

## S1 Materials and Characterization

### Materials:

Indium(III) nitrate hydrate ( $\text{In}(\text{NO}_3)_3 \cdot 5\text{H}_2\text{O}$ ) was purchased from Sinopharm chemical reagent Co. Ltd. 4,4',4'',4'''-(1,4-phenylenebis(pyridine-4,2,6-triyl))tetrabenzoic acid (**H4L**) was synthesized according to literature.<sup>1</sup> Styrene oxide were supplied by Heowns (China) Biochem technologies. All the other chemicals were purchased from Hengshan chemical corporation without further purification.

### Characterization:

Powder X-ray diffraction (PXRD) was recorded on Ultima IV (Rigaku) with Cu  $K\alpha$  radiation. Thermogravimetric analysis (TGA) were performed on TG 209 (NETZSCH) under  $\text{N}_2$  atmosphere. X-ray photoelectron Spectrometer (XPS) analysis was carried out on an Axis Ultra DLD (Kratos Analytical Ltd.) spectrometer, internal standard carbon was 284.8 eV. Solid-state photoluminescent spectra was measured by F-4500 FL Spectrophotometer (Hitachi) at room temperature. Scanning electron microscope (SEM) images were captured by SU3500 (HITACHI). Field emission scanning electron microscope (FESEM) images were obtained by MERLIN Compact (ZEISS).  $^1\text{H}$  NMR and  $^{13}\text{C}$  NMR spectra were recorded in  $\text{CDCl}_3$  on 400 MHz spectrometer (ASCEND 400, Bruker). Chemical shifts are reported in ppm from tetramethylsilane with the solvent resonance as the internal standard. Yield was measured on GC analysis (Fuli instruments) using 1,3,5-trimethoxybenzene as the internal standard, which equipped with a flame ionization detector (FID) and an OV 1701 column.

$$\text{Yield} = \frac{\text{Moles of target carbonate}}{\text{Theoretical moles of target carbonate}} \times 100\%$$

Inductively coupled plasma mass spectrometer (ICP-MS) was carried out with IRIS Advantage (Thermo). After reaction completed, the reaction mixture was centrifuged at 10000 rpm for 10 minutes. Then, 20  $\mu\text{L}$  supernatant liquid was digested with 10 mL aqua regia. After cooling to room temperature, the mixture was transferred to a 50 mL volumetric flask and diluted to 50 mL. The obtained sample was tested using ICP analysis.

## S2 Experimental Section

**Preparation of  $\{(\text{NH}_2(\text{CH}_3)_2) [\text{In}(\text{L})] \cdot 2\text{DMF} \cdot \text{H}_2\text{O}\}_n$  (**V103**).**  $\text{In}(\text{NO}_3)_3$  (10 mg) and **H4L** (10 mg) were dissolved in DMF and placed in a 25 mL Teflon-lined stainless autoclave. After added 200  $\mu\text{L}$   $\text{HNO}_3$  and 0.1 mL  $\text{H}_2\text{O}$  as the modifier, the autoclave was sealed and heated at 120  $^\circ\text{C}$  for 24 hours under autogenous pressure. After cooling to room temperature, light yellow block crystals were obtained. Elemental analysis (%) calculated for compound **V103**: C 60.4, H 4.64, N 6.77. Found: C 59.6, H 4.52, N 6.91. CCDC number: 1830480.

### **Catalyzed cycloaddition reaction:**

In a typical experiment, 20 mg (~0.02 mmol) **V103**, 2.0 mmol styrene oxide, 20  $\mu$ L water (if needed) and 20 mg TBAB were mixed in a glass tube. The reaction tube was purged with CO<sub>2</sub>, and kept in CO<sub>2</sub> environment by a balloon. The reaction was kept magnetically stirred at 60 °C for a given time. After that, the reaction solution was filtered through a filter membrane (0.22  $\mu$ m) to remove the solid particles, and further purified by silica gel column to remove the inorganic or organic salts. Then, the mixture solution was analyzed by gas chromatography (GC) using 1,3,5-trimethoxybenzene as the internal standard, <sup>1</sup>H NMR and <sup>13</sup>C NMR spectra. In the cycloaddition reaction for other epoxides, we keep the substrates at the same equivalent. For the substrate propylene oxide, and 1,2-epoxybutane, the reactions were carried out in a stainless autoclave.

**Recyclability of the catalyst:** When the reaction was complete, the catalyst and product was isolated by centrifugation at 10000 rpm for 10 minutes. The liquid phase was removed with a syringe to ensure that the product and any starting materials were removed as completely as possible. Then the catalyst was washed with alcohol three times, and dried at room temperature. With the addition of fresh substrate, water and TBAB, a new reaction could be conducted as same as the initial run.

### **X-ray Structure Determination:**

The crystallographic measurement was measured on a SuperNova Single Crystal Diffractometer equipped with a graphite-monochromatic Mo-K $\alpha$  radiation ( $\lambda = 0.71073$  Å). The structure was solved by direct methods and refined to convergence by least squares method on F<sup>2</sup> using the SHELXTL (olex 2) software suit.<sup>2,3</sup> All non-hydrogen atoms are refined anisotropically. The inner structure is isoccupied by seriously disordered solvent molecules, and some attempts to locate and refine were unsuccessful. To solve this problem, we used PLATON/SQUEEZE to remove the highly disordered solvent molecules, and the final molecular was demined by combination of TG analysis and elemental analysis. Detailed crystal data and structure refinements for **V103** are shown in Table S1.

### **S3 References**

- (1). J. H. Wang, Y. Zhang, M. Li, S. Yan, D. Li and X. M. Zhang. *Angew. Chem. Int. Ed.*, 2017, **56**, 6478–6482.
- (2). O. V. Dolomanov, L. J. Bourhis, R. J. Gildea, J. A. K. Howard and H. Pushmann. *J. Appl. Crystallogr.* 2009, **42**, 339-341.
- (3). G. M. Sheldrick. *Acta Crystallogr., Sect. A: Fundam. Crystallogr.* 2008, **64**, 112-122.

**Table S1** Crystal data and structure refinement for **V103**

Identification code	<b>V103</b>
Empirical formula	C <sub>46</sub> H <sub>34</sub> InN <sub>3</sub> O <sub>9</sub>
Formula weight	887.58
Temperature / K	293(2)
Crystal system	Orthorhombic
Space group	Pcca
<i>a</i> / Å	11.033(2)
<i>b</i> / Å	12.713(3)
<i>c</i> / Å	36.597(7)
$\alpha$ / °	90
$\beta$ / °	90
$\gamma$ / °	90
Volume / Å <sup>3</sup>	5133.3(19)
<i>Z</i>	4
$\mu$ / mm <sup>-1</sup>	0.509
<i>F</i> (000)	1808.0
Goodness-of-fit on <i>F</i> <sup>2</sup>	1.182
Final R indexes [ <i>I</i> ≥ 2σ( <i>I</i> )]	<i>R</i> <sub>1</sub> = 0.0895, <i>wR</i> <sub>2</sub> = 0.2413
Final R indexes [all data]	<i>R</i> <sub>1</sub> = 0.1175, <i>wR</i> <sub>2</sub> = 0.2604

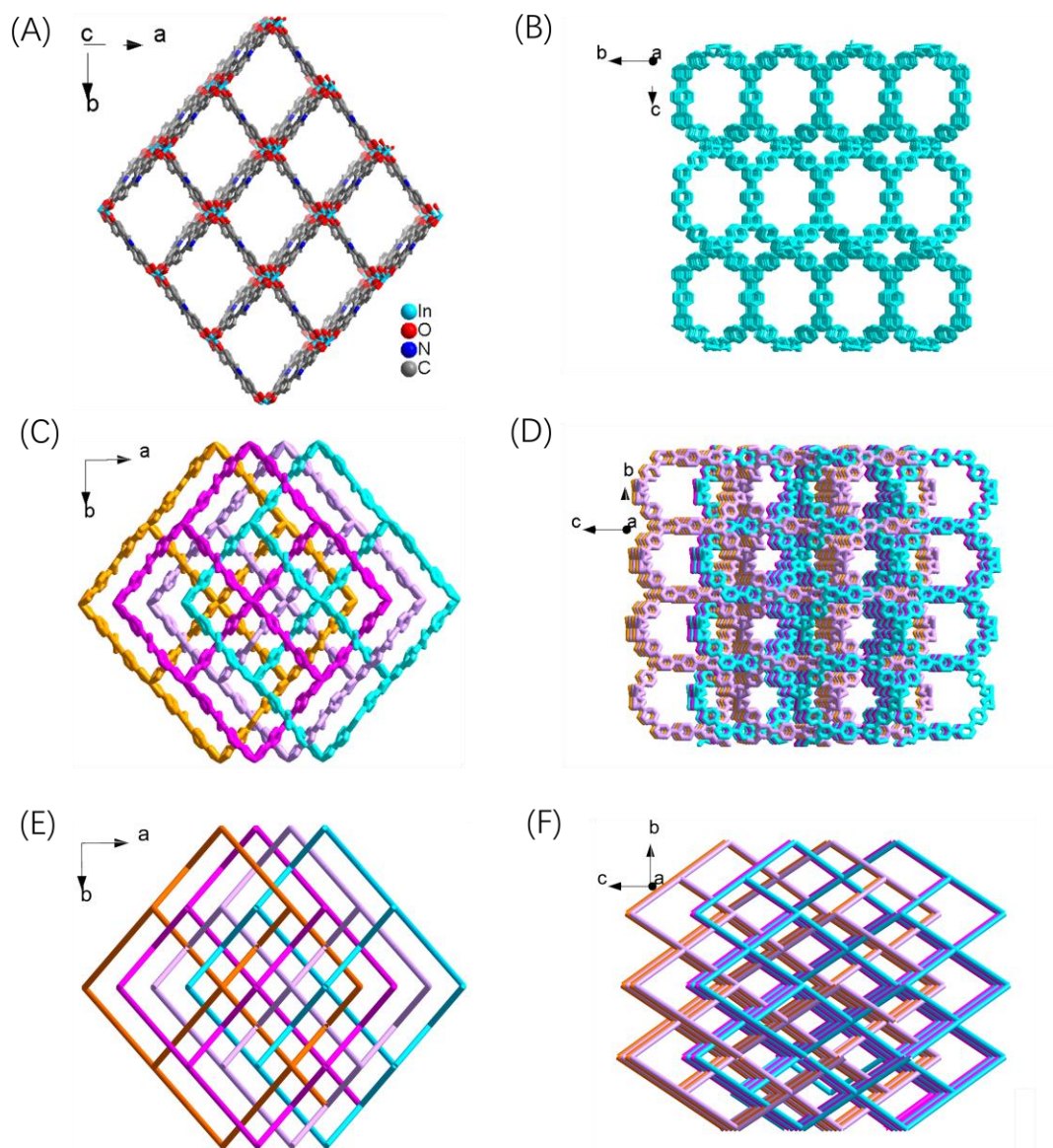


Figure S1. (A) View of the single network in **V103** along the *c* direction. (B) View of the single network in **V103** along the *a* direction. (C) The 3D four-fold interpenetrated framework of compound **V103** along the *c* direction. (D) The 3D four-fold interpenetrated framework of compound **V103** along the *a* direction. (E) The simplified topology network of **V103** along the *c* direction. (F) The simplified topology network of **V103** along the *a* direction.

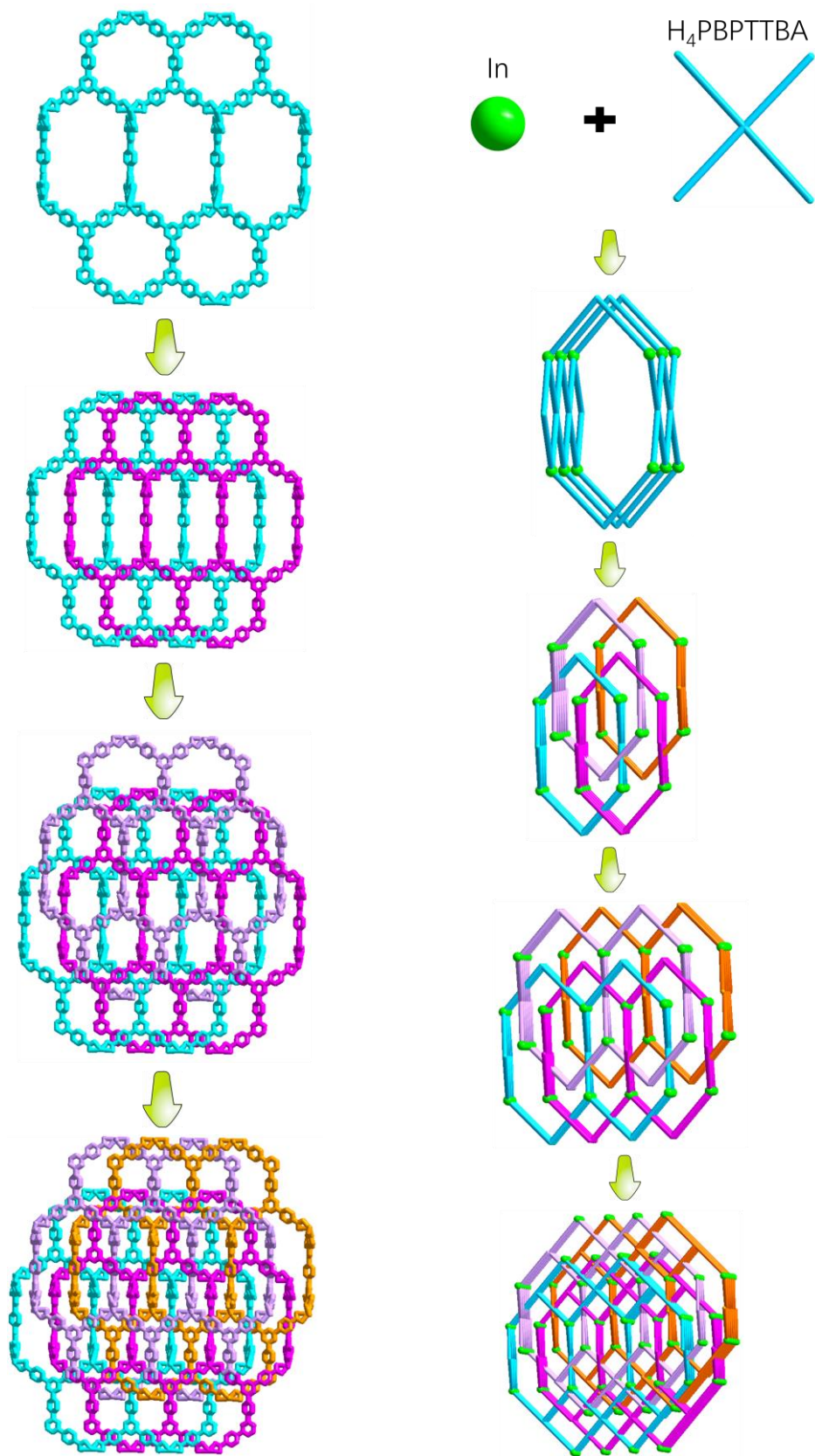


Figure S2. Left: the formation process of the 4-fold Interspersed framework **V103**. Right: simplified topology network of the formation process of **V103**.

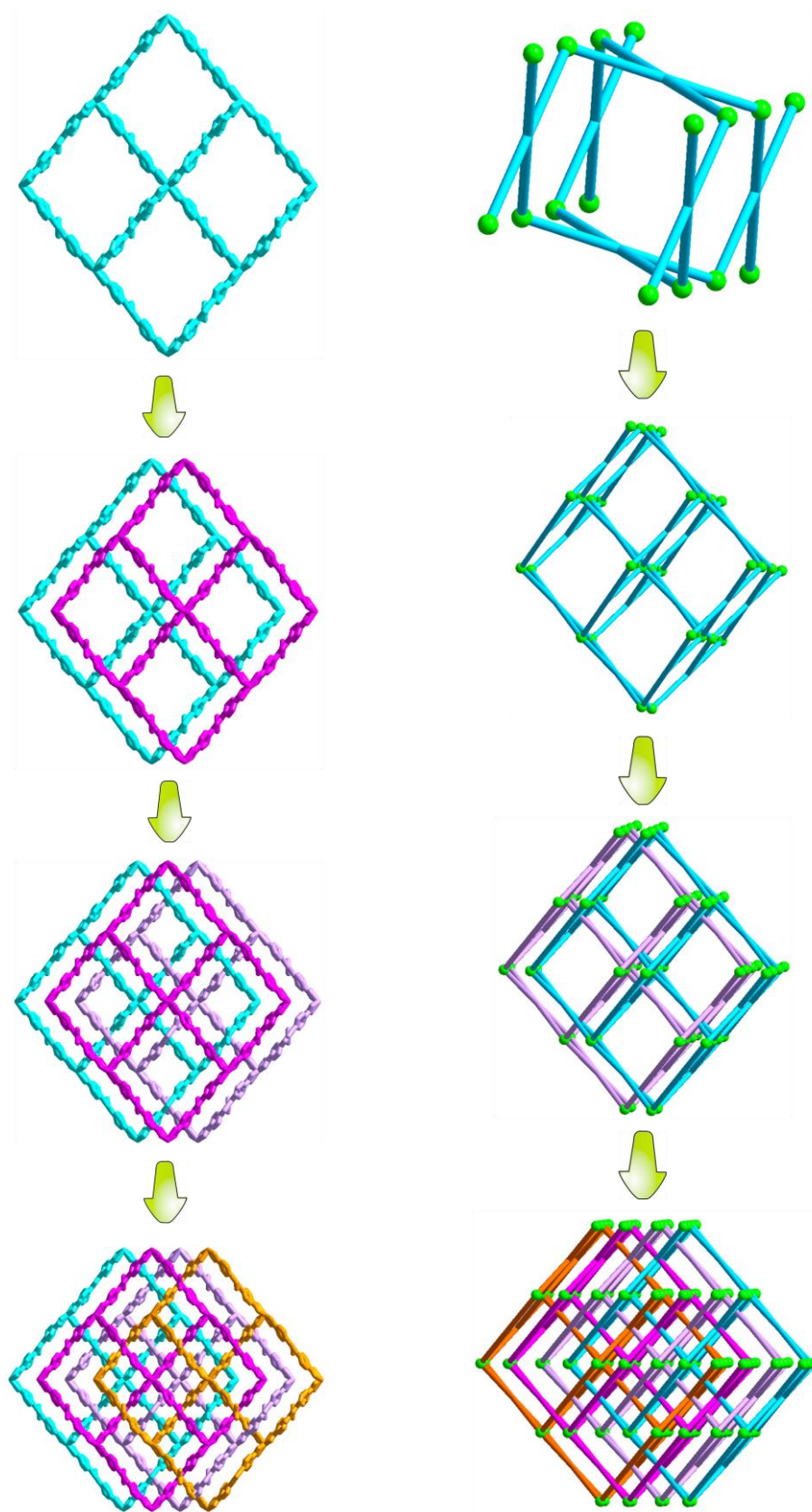


Figure S3. Left: the formation process of the 4-fold Interspersed framework **V103** along the  $c$  direction. Right: simplified topology network of the formation process of **V103** along the  $c$  direction.

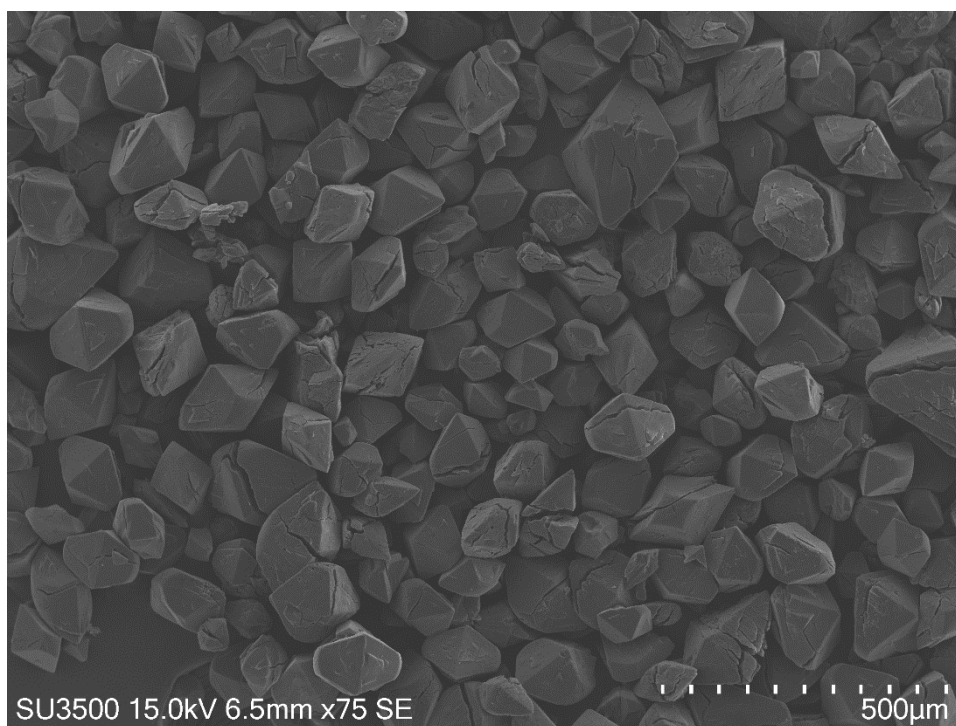


Figure S4. SEM image of as-synthesized compound **V103**.

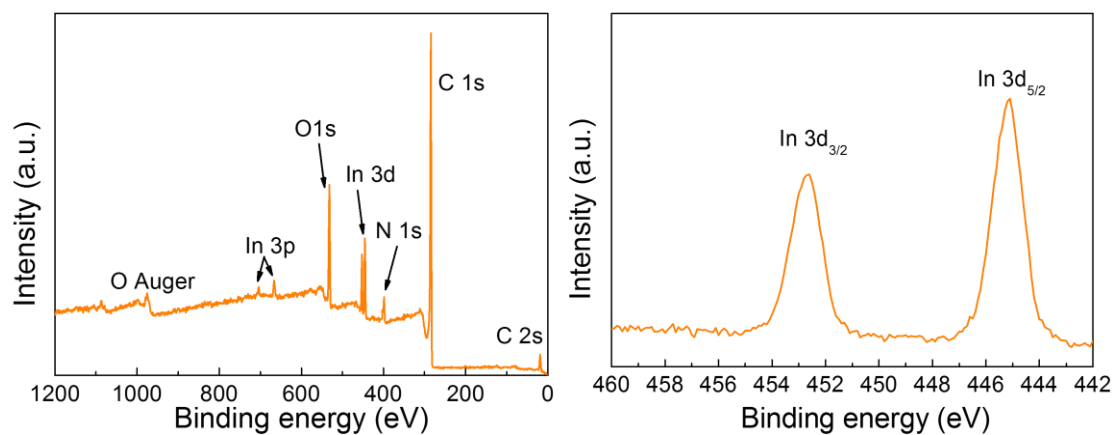


Figure S5. XPS spectra of as-synthesized **V103**. The binding energies for In 3d<sub>3/2</sub> and 3d<sub>5/2</sub> in the frameworks of **V103** are found to be 452.6 eV and 445.2 eV, respectively, which is concordant with the In<sup>3+</sup> at 452.4 eV and 444.8 eV. These results demonstrate that In is trivalence in the frameworks.

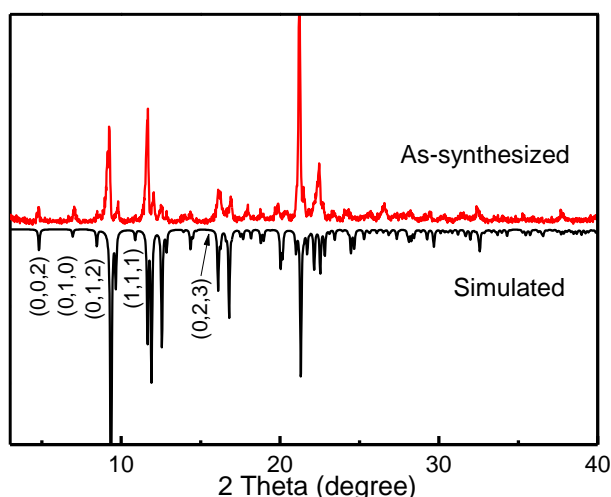


Figure S6. PXRD patterns of as-synthesized compound **V103** and simulation.

It should be pointed out that the as-synthesized pattern was measured directly after washed by DMF without further drying. As shown in Figure S6, the as-synthesized pattern is matched well with the simulated one. The intensity ratios for various peaks in PXRD patterns are related to the crystal orientation (Crystal shape is the macroscopical phenomenon), which is determined by the growth rate of different directions. The crystal growth rate is affected by many factors, such as reaction temperature, substrate concentration, residual impurity, and acid-base environment. These factors lead to the obtained crystals have different shapes. Therefore, some peaks in the experimental pattern maybe have different intensity from those observed in the simulated pattern.

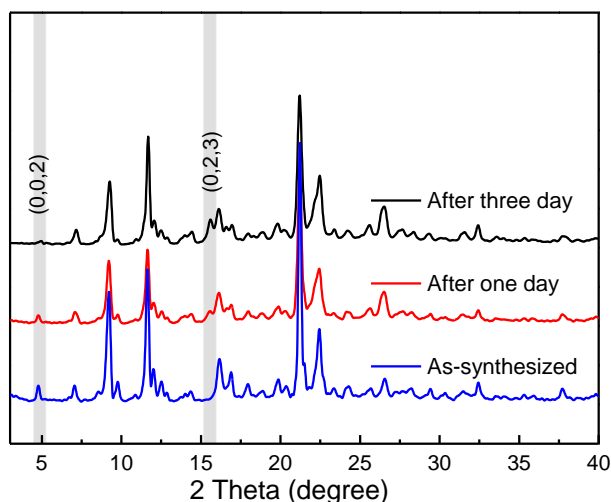


Figure S7. Powder XRD patterns of as-synthesized compound **V103** drying in air.

We also find that the as-synthesized PXRD patterns slightly change with time increasing after drying in air. As shown in Figure S7, the intensity of peak at  $2\theta = 4.8^\circ$  (002 direction) decreases after drying in air, and the weak satellite peak at  $2\theta = 15.5^\circ$  (023 direction) starts to appear with time going on (Figure S7). These changes maybe originate from the removal of solvents in the large channels.

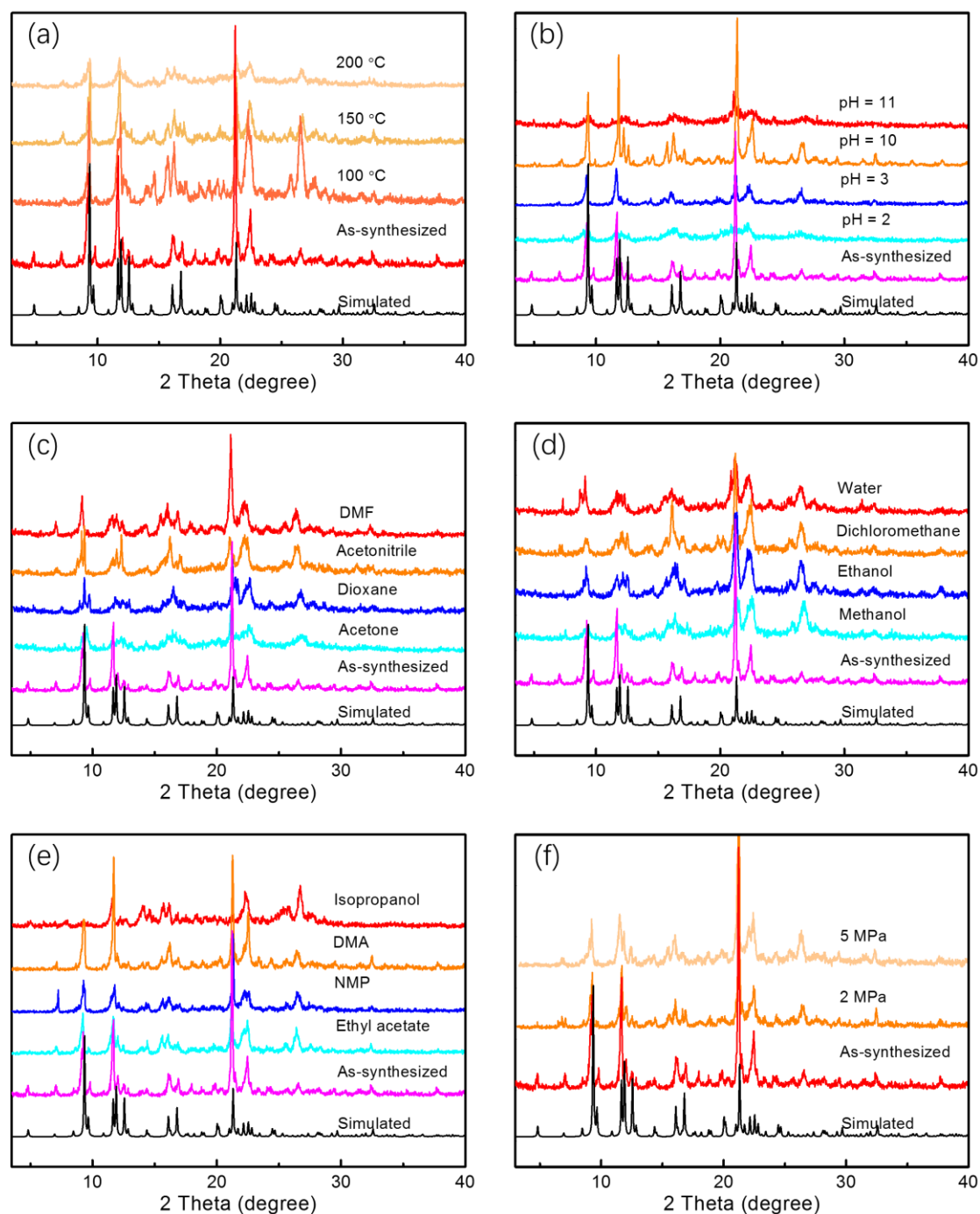


Figure S8. Stability investigations on compound **V103**. (a) The PXRD patterns of compound **V103** after heating 3 h at different temperature. (b) The PXRD patterns of compound **V103** after immersing in different pH solvents for 12 hours. (c, d, e) The PXRD patterns of compound **V103** after immersing in different solvents for 12 hours. (f) The PXRD patterns of compound **V103** after treating with Ar for 12 hours.

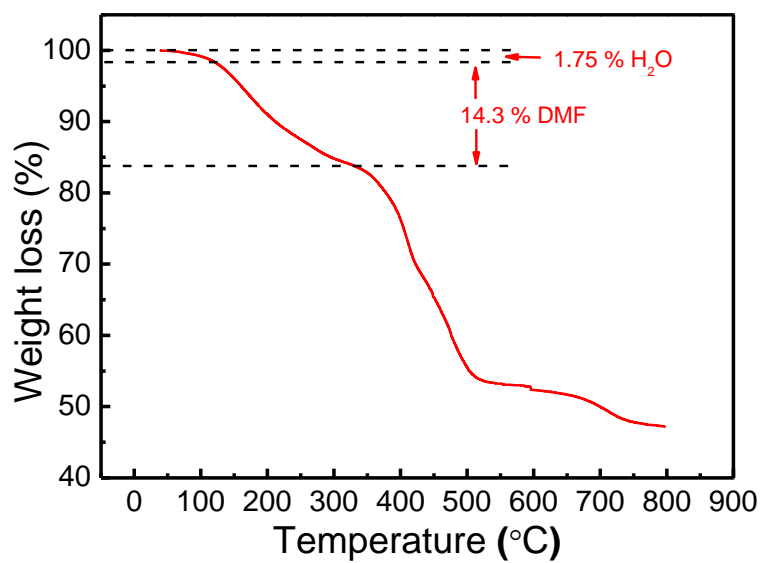


Figure S9. Thermogravimetric analyses curves of as-synthesized **V103**.

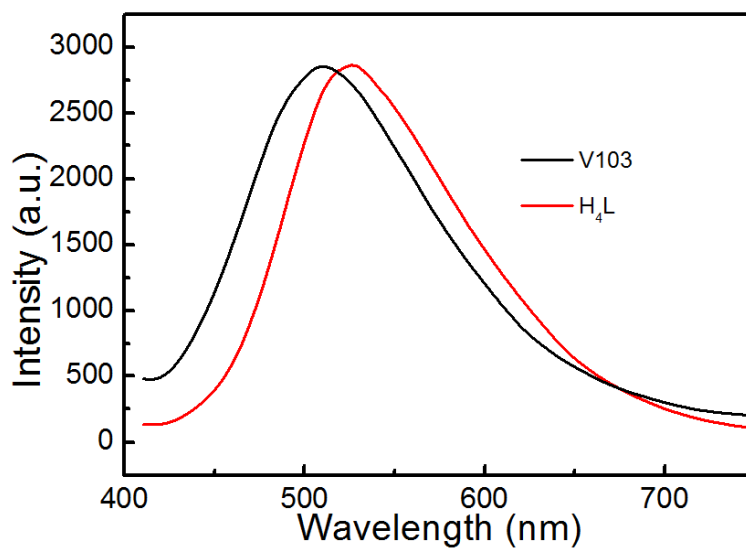


Figure S10. Solid-state photoluminescent spectra of free ligand **H<sub>4</sub>L**, **V103**.

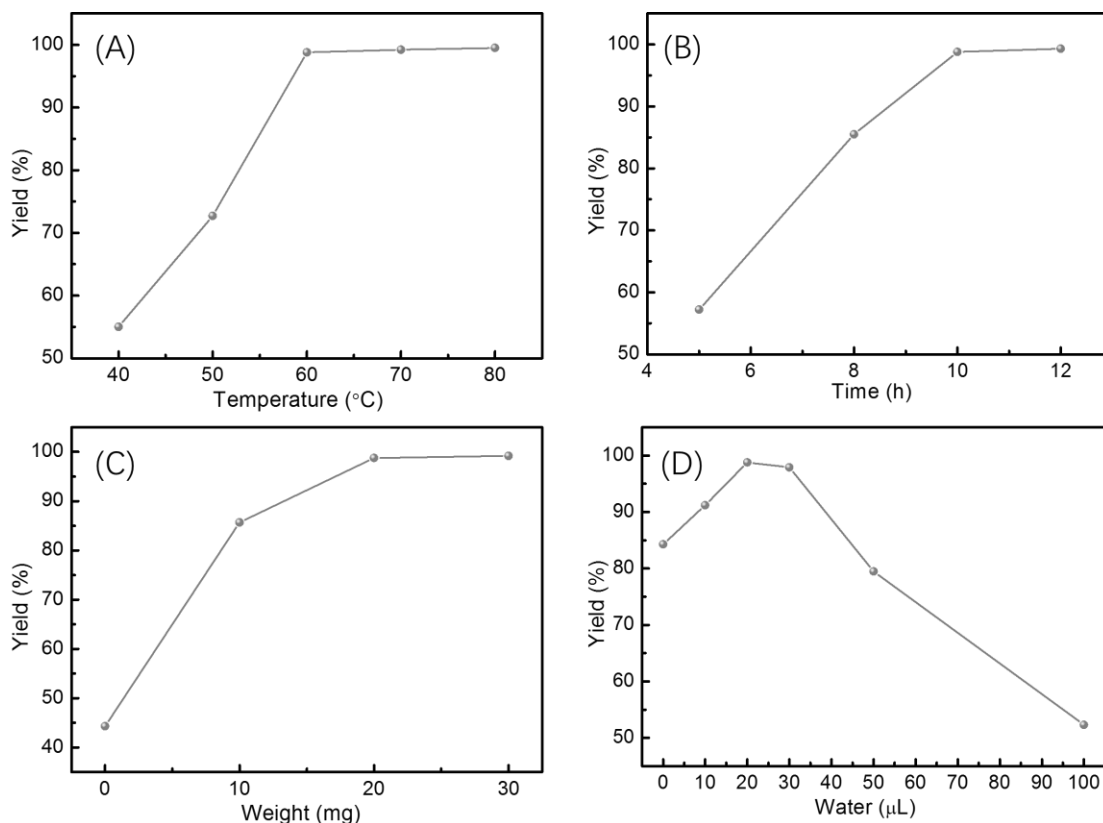


Figure S11. The effect of reaction conditions on the CO<sub>2</sub> cycloaddition reaction. A: Reaction temperature. B: Reaction time. C: Catalyst weight. D: Various amount of water. Reaction conditions: 1 bar CO<sub>2</sub> (balloon), styrene oxide 2 mmol, 20 mg TBAB.

The effect of reaction conditions on the CO<sub>2</sub> cycloaddition reaction were investigated, and the results are recorded in Figure S11. The yield of styrene oxide increases with temperature in the low temperature range, and turned independent after 60 °C (Figure S11-A). This is understandable because the reaction is almost completed at 60 °C, and the effect of higher temperature is very limited for this reaction. With time increasing, the reaction yield reached to ~99% at 10 hours. Further extension of reaction time has no effect on the yield, indicating the appropriate reaction time is 10 hours. When the reaction only catalyzed by the cocatalyst TBAB, the yield is poor. But it increased significantly after added catalyst **V103** in the reaction mixture, which revealing that compound **V103** is an efficient catalyst in this cycloaddition reaction. Furthermore, the effect of various amounts of water was also explored. When adding trace of water into the reaction mixture, the reaction is accelerated by water and the yield is increased to ~99% with 20 μL water after 10 hours. However, the yield is decreased seriously with further increased the amount of water above 30 μL. These suggesting that different amount of water have diverse effects on the CO<sub>2</sub> cycloaddition reaction, and the appropriate amount of water is 20 μL.

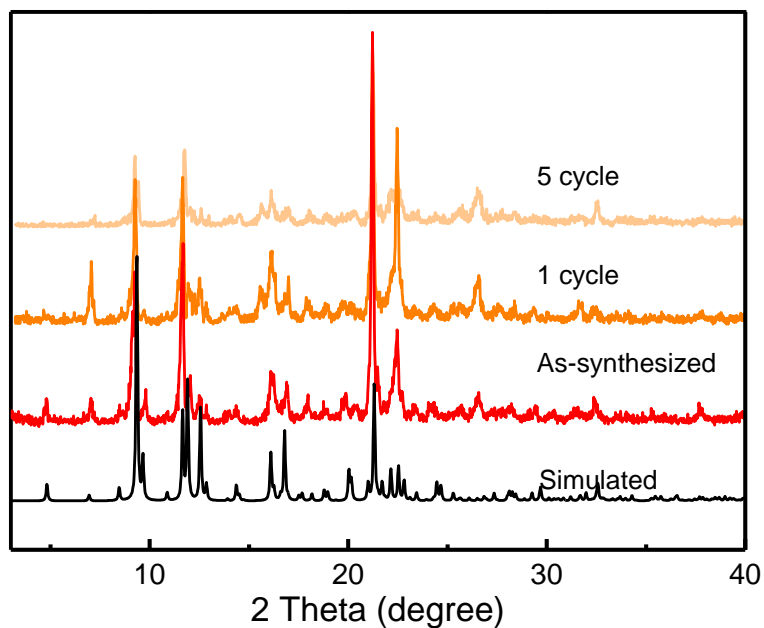


Figure S12. The PXRD patterns of compounds **V103** after five cycles. After five cycles, the experimental PXRD patterns are in good agreement with the as-synthesized and simulated ones, suggesting **V103** have an excellent stability in the CO<sub>2</sub> cycloaddition reaction.

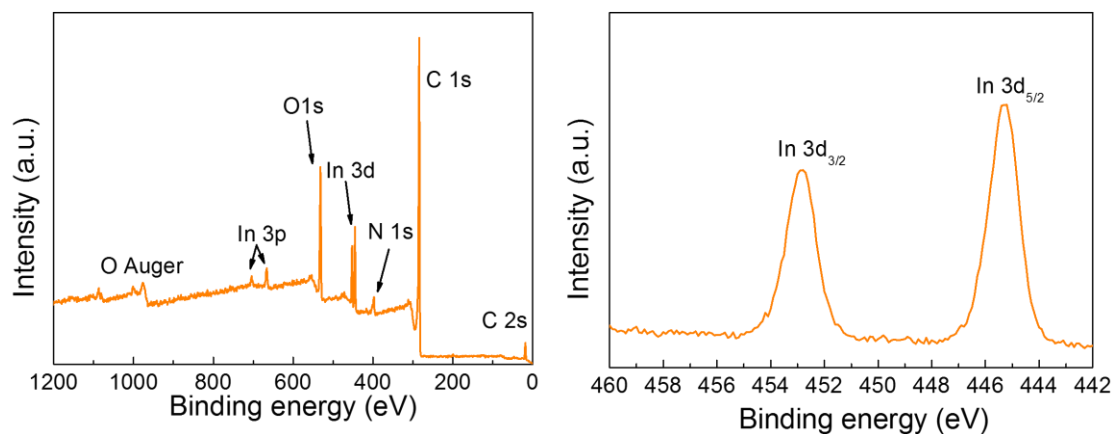


Figure S13. XPS spectra of **V103** after five cycles. The binding energies for In 3d<sub>3/2</sub> and 3d<sub>5/2</sub> are found to be 452.3 eV and 445.3 eV, respectively, which is concordant with the initial ones, indicating that **V103** is keep stable during the reaction.

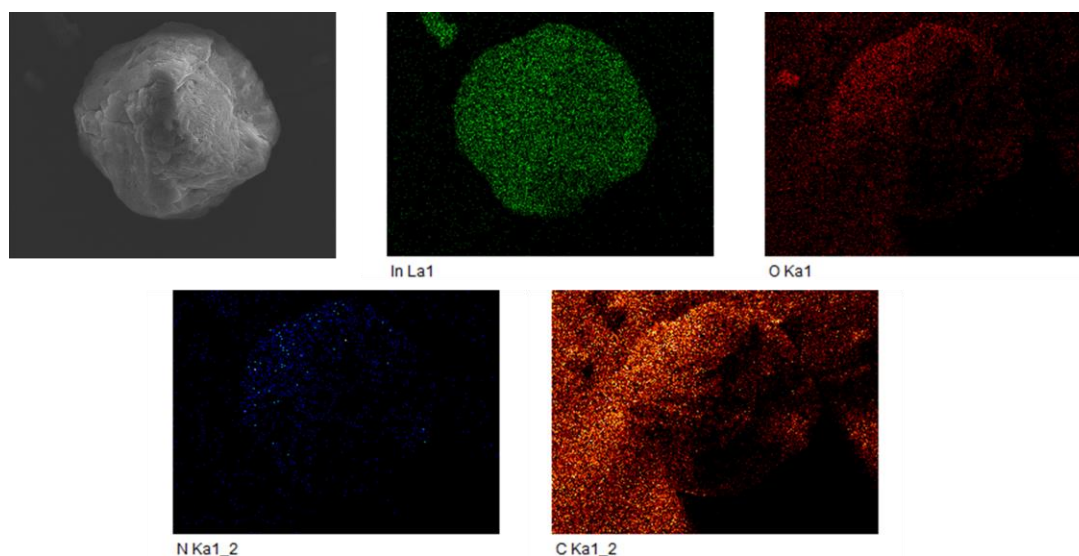


Figure S14. Field emission scanning electron microscope (FESEM) image of crystal **V103** after five cycles and corresponding energy-dispersive X-ray spectroscopy (EDS) element mapping images. The elements C, N, O, and In are uniformly distributed, indicating the crystal framework is not collapsed.

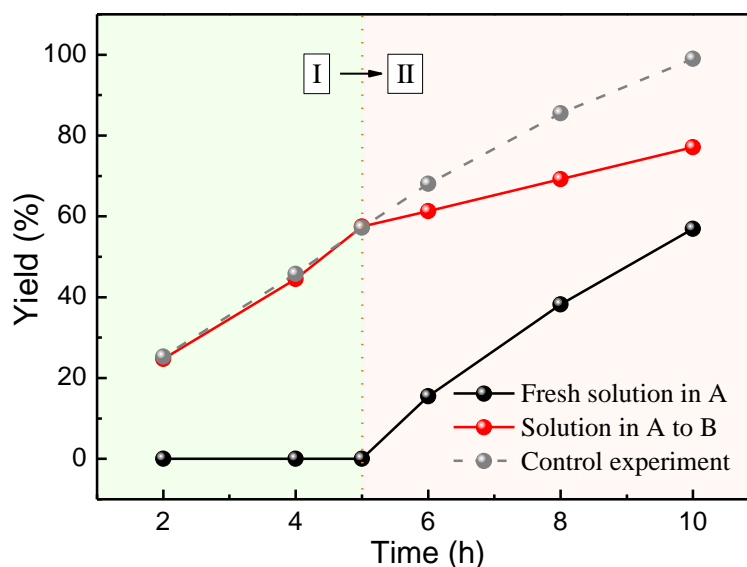


Figure S15. Catalyst filtration test experiment for the cycloaddition of  $\text{CO}_2$  with styrene oxide catalyzed by **V103**. A reaction tube **A** was charged with TBAB, styrene oxide and **V103**. The mixture was reacted under given conditions and monitored by GC analysis. (I) When the reaction in tube **A** reacted after 5 h, the solution in **A** was removed by centrifugation and added into a new tube **B**. A fresh solution of starting material was added in tube **A** where the catalyst **V103** remained. Both tube **A** and **B** were then reacted under the same conditions and monitored by GC analysis. (II) The yield in tube **B** increased slowly, whereas reaction was rapidly reacted in tube **A** (light-pink section). Indium leaching result (solution in tube **B**) was measured, and no  $\text{In}^{3+}$  was detected by ICP analysis. This result demonstrated that **V103** was heterogeneous catalysis in nature.

Conditions: 1 bar CO<sub>2</sub> (balloon), 20 mg **V103**,  $T = 60\text{ }^{\circ}\text{C}$ , styrene oxide 2 mmol, 20 mg TBAB, 20  $\mu\text{L}$  water.

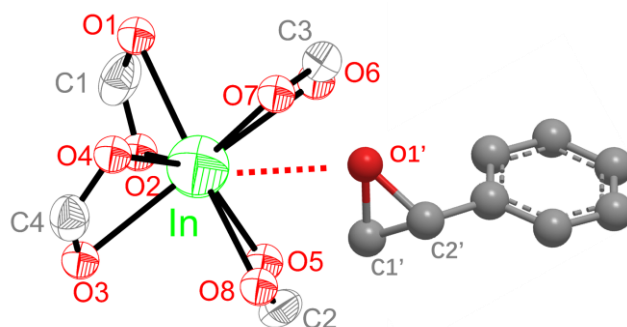


Figure S16. The scheme for the interaction between In node and epoxide

In compound **V103**, there exist a large open channel with diameter of 8.6 Å along  $a$  direction, which is large enough to enrich substrate molecules. On the other hand, the residual spaces among coordinated carboxyl (For example: O<sub>7</sub>...O<sub>8</sub> distance = 3.124 Å, O<sub>5</sub>...O<sub>6</sub> distance = 3.062 Å, C<sub>3</sub>...C<sub>2</sub> distance = 4.064 Å,  $\angle\text{C}_3\text{InC}_2 = 100.0^{\circ}$ ) are sufficient to allow the O atom of epoxide molecules (O<sub>1</sub>'...C<sub>1</sub>' distance = 1.541 Å) interacting with the Lewis acidic centers (In<sup>3+</sup>). Hence, the substrate could be transported through the MOF framework and interact with In node.

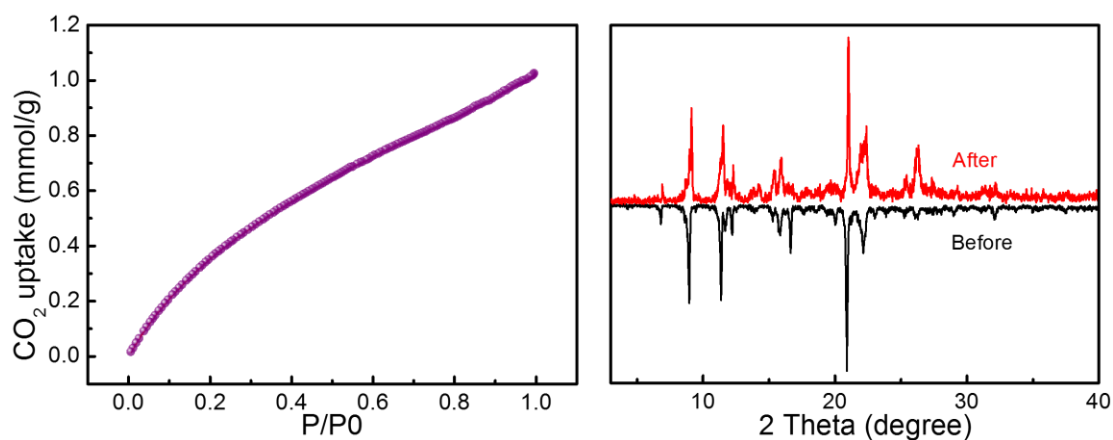


Figure S17. Left: CO<sub>2</sub> adsorption isotherms of **V103**. Right: The corresponding PXR patterns of compounds **V103** after CO<sub>2</sub> adsorption.

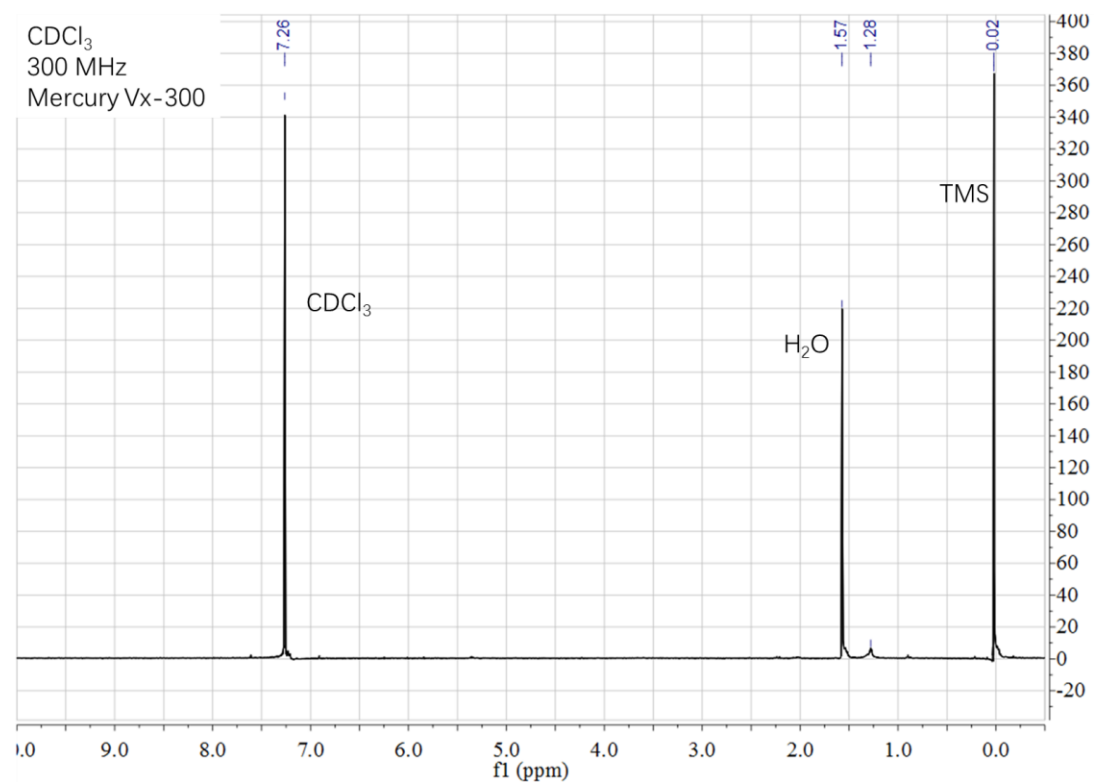


Figure S18. <sup>1</sup>H NMR (400 MHz) spectrum of CDCl<sub>3</sub>

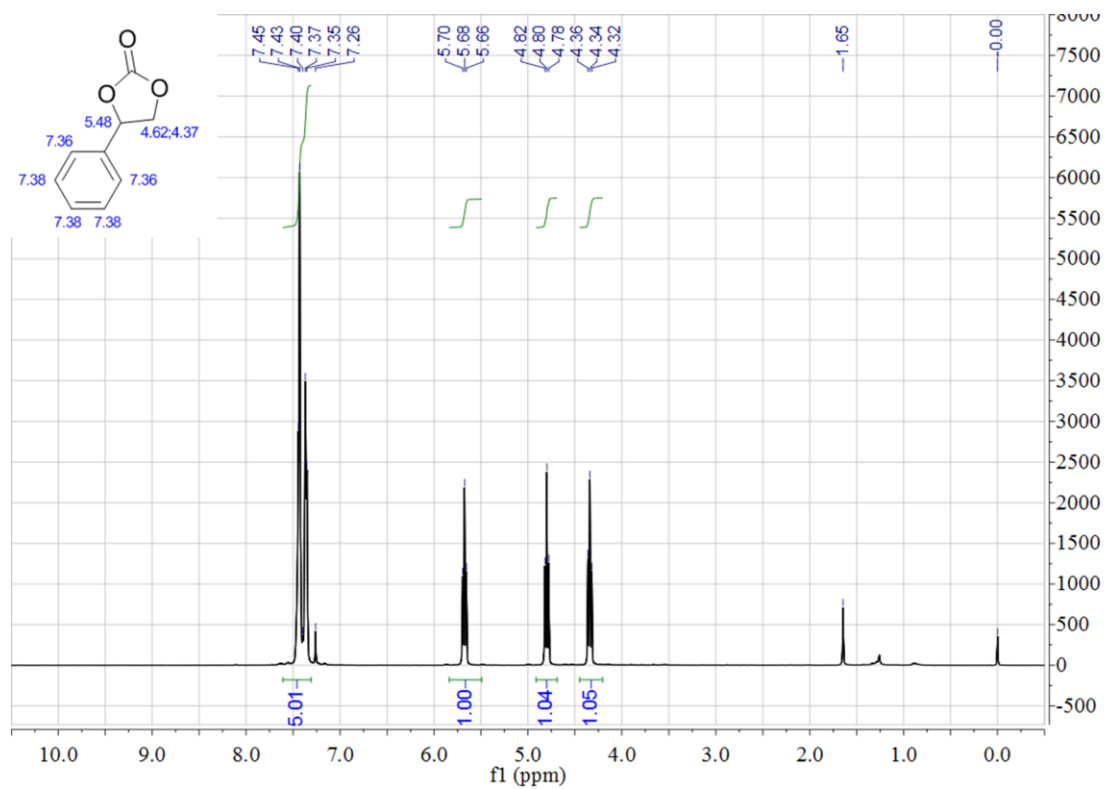


Figure S19. <sup>1</sup>H NMR (400 MHz, CDCl<sub>3</sub>) spectrum of styrene carbonate

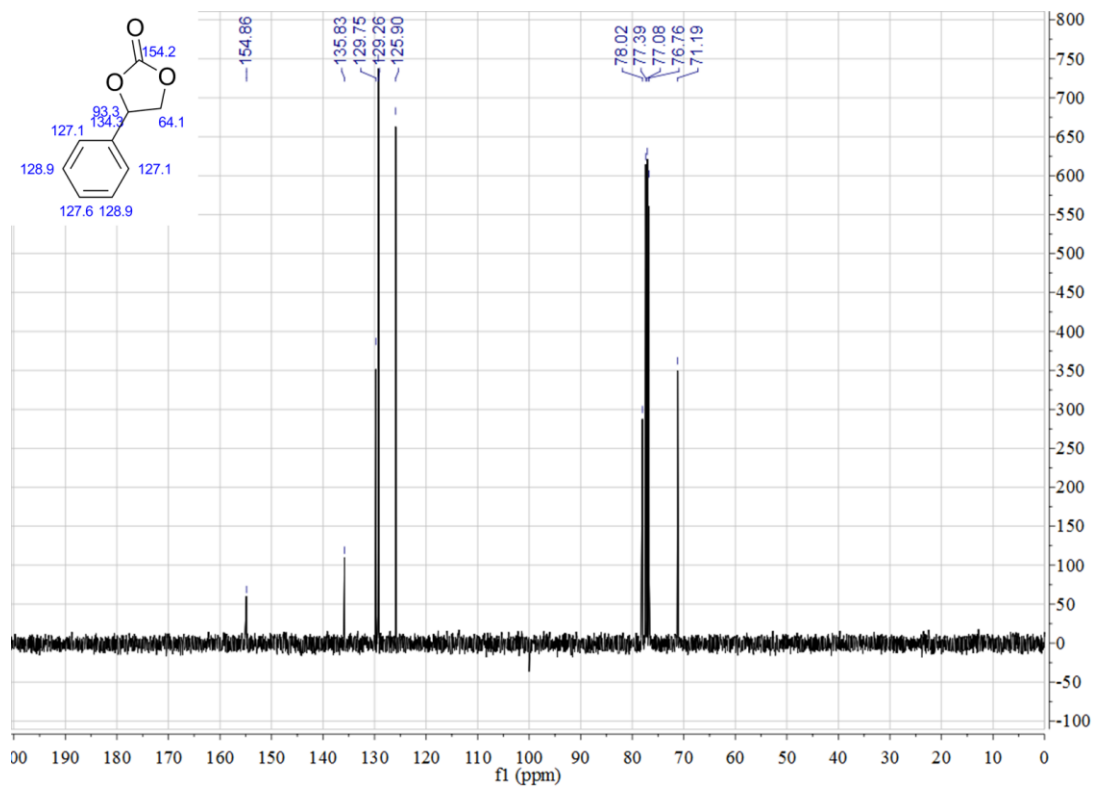


Figure S20.  $^{13}\text{C}$  NMR (400 MHz,  $\text{CDCl}_3$ ) spectrum of styrene carbonate

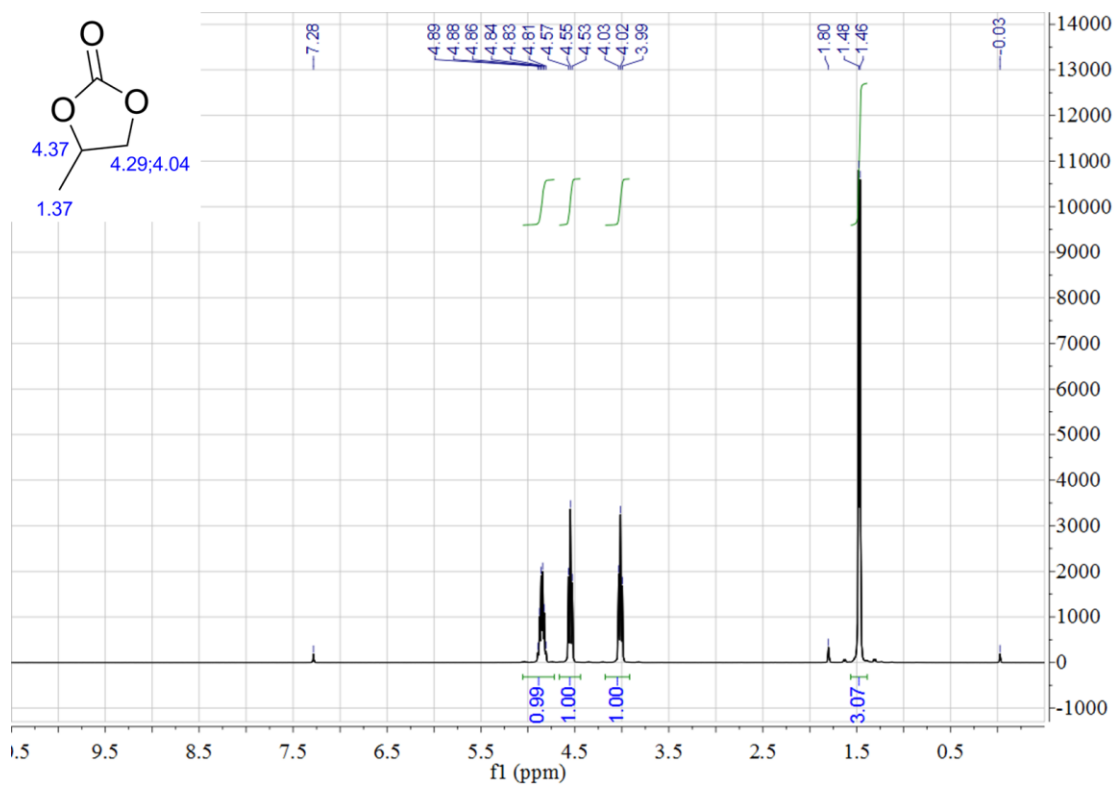


Figure S21.  $^1\text{H}$  NMR (400 MHz,  $\text{CDCl}_3$ ) spectrum of propylene carbonate

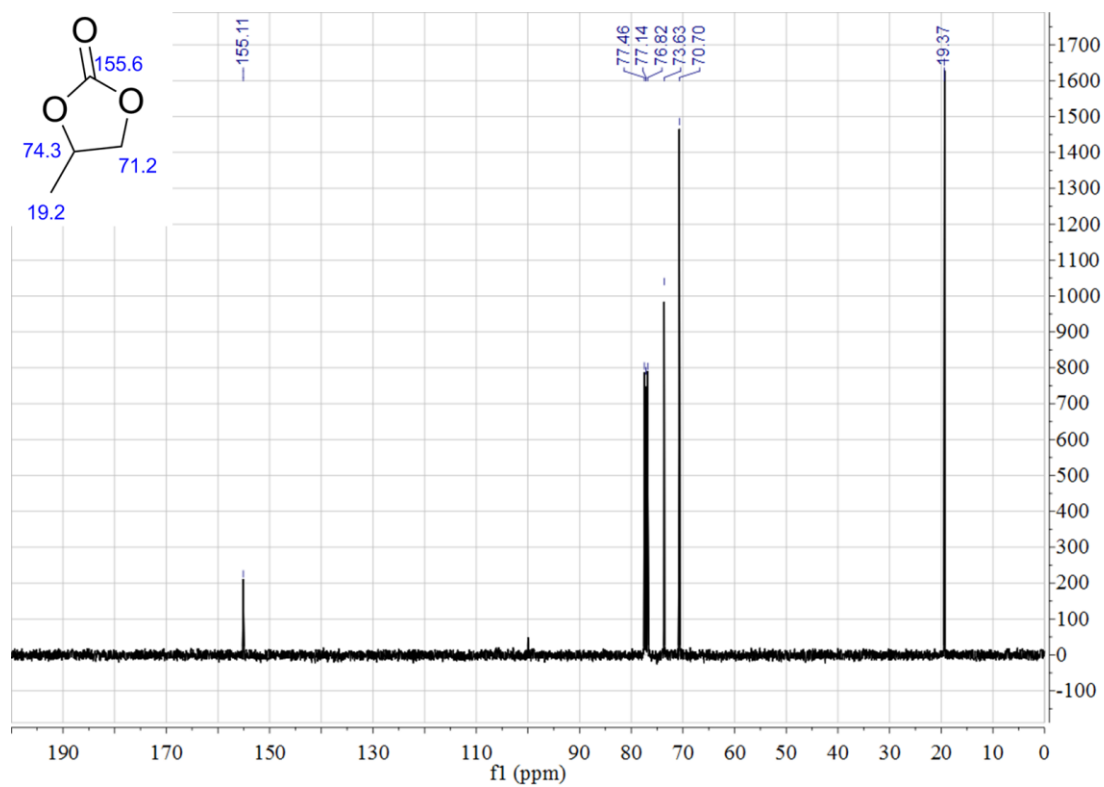


Figure S22.  $^{13}\text{C}$  NMR (400 MHz,  $\text{CDCl}_3$ ) spectrum of propylene carbonate